Experimental Study of a Photovoltaic Direct Current Water Pumping System for Irrigation in Rural-Isolated Region of Arequipa, Peru

Aixa Anel Peralta Vera
Universidad Tecnológica del Perú,
Av. Tacna y Arica 160,
Arequipa 04000, Peru

Herbert Jesús del Carpio Beltrán
Universidad Tecnológica del Perú,
Av. Tacna y Arica 160,
Arequipa 04000, Peru

Juan Carlos Zúñiga Torres
Universidad Tecnológica del Perú,
Av. Tacna y Arica 160,
Arequipa 04000, Peru

Juan José Milón Guzmán
Universidad Tecnológica del Perú,
Av. Tacna y Arica 160,
Arequipa 04000, Peru

Sergio Leal Braga
Pontifícia Universidade
Católica do Rio de Janeiro,
Rio de Janeiro 38097, Brazil

In the present experimental study, a photovoltaic (PV)-powered system in continuous current (4 kW) for the pumping of water in an isolated, rural agricultural zone in Arequipa—Peru was analyzed. A meteorological station was installed in the studied zone, measuring solar radiation, temperature, relative humidity, and wind speed. The electrical and hydraulic parameters of the solar-pumping system (i.e., electric current, voltage, mass flow, and hydraulic pressure) were measured in order to evaluate the efficiency of the energy transformation processes. The results indicate that, during the year of 2017, the PV pumping system in direct current (DC) functions from 07 h 30 min to 15 h 30 min, during an average of 8 h a day. The PV array, hydraulic, and global efficiencies were evaluated. This allows for the interpretation of efficiency independent of solar irradiance. The efficiency of the PV array and global efficiency remained constant (11.5% f and 8.5%, respectively). The functioning interval of the PV array ranges from 880 W up to 3400 W, making evident the versatility of the system of generation and consumption in DC, which is able to function since solar irradiance is at least 200 W/m², corresponding to 880 W of PV array power, 27 m of total dynamic head (TDH) and 2 kg/s of mass flow, and 70% hydraulic efficiency. With greater mass flows (6.3 kg/s), the PV array power was 3256 W with a hydraulic efficiency of 55%, a TDH of 30 m, and a peak solar irradiance of 1190 W/m². When the whole system functions in DC, the efficiencies are superior to those of systems, which operate with DC/alternating current (AC) current inverters. [DOI: 10.1115/1.4042724]

Keywords: photovoltaic pump, isolated communities, continuous current, pulse wave

1 Introduction

Electrical power is an indispensable resource for any population, responsible for increasing the development of economic activities and improving the general quality of life [1]. The rural zones of Latin America have favorable geographic and climatic conditions for the generation of electric power from solar energy, using photovoltaic (PV) systems. However, the use of this renewable source is currently not widespread in the region, mainly due to economic and cultural factors, such as unfamiliarity with the technology. For this reason, it is necessary to extend collective knowledge concerning photovoltaic technology in order to promote its exploitation and benefit isolated communities, improving their life conditions.

This study has been carried on in "Majes Tradición," a winery located in the Santa Rosa irrigation zone, part of *Viñas del Ocho* vineyards, located in Uraca—Castilla, Arequipa, Peru (16°13′35.30″ S; 72°27′04.49″ W). This vineyard extends over 12 ha of land, dedicated exclusively to the cultivation of different strains of grapevine as well as their distillation for the production of wine and pisco (grape spirit). The water for *Majes Tradición* winery comes from a natural water source originated in the Majes River, and located at a distance of 1500 m and 65 m below the main winery water reservoir. The vineyards are located in an originally arid zone: water is transported to the vineyards through man-made channels, which is why they are considered an extension of the agricultural zone of the region. Transporting water to the vineyards and the winery has proven to be a challenge for the company, and so is the low quality and high cost of electrical power. These two problems affect the grape production and the transformation processes for wine and *Pisco* making, but the latest generates a negative environmental impact, since the company uses petroleum-based fuels regularly for its production activities.

The main goal of this research project is to conduct an experimental study of the generation of electrical power, using a photovoltaic energy system in continuous current for water pumping.

2 Solar Pumping Systems in Isolated Communities

Arequipa is one of the regions of Peru that receive the highest solar radiation and benefit from the greatest number of sunlight hours per year. This region has a great quantity of rural zones whose inhabitants specialize in textile, agricultural, and cattle-raising activities, mainly. Electricity, fuel, and water are necessary for the development of these zones, but currently most of them are not connected to the energy grid. The lack of electrical power forces these isolated rural zones to use petroleum-based fuels to generate electricity. One of the advantages of diesel-powered, water pumping systems is that the installation is simple. Nevertheless, the disadvantage arises with the frequent need for maintenance of the equipment, constant fuel consumption, indiscriminate use of nonrenewable resources, and environmental pollution caused by exhaust gases [2]. On the other hand, the dry nature of Arequipa's climate constitutes a challenge for

agriculture, one of the main activities of isolated rural zones. This situation creates a necessity for the optimization of irrigation systems, which would increase the yield in the process of planting and harvesting, and the income of the population [3]. Moreover, the lack of governmental support for the development of solutions generates uncertainty and causes migration from the countryside to the city. To face these social, economic, and environmental issues, photovoltaic systems adapted to the climatic characteristics of the region are an economic, reliable, and eco-friendly alternative [4,5]. For example, these systems can contribute to the expansion of the electrical power grid in the distant regions [6], which would allow the development of different economic activities, such as agricultural irrigation or cattle raising [7], at lower costs [8].The use of photovoltaic energy brings with it economic, social, and environmental benefits, providing the population with access to telecommunication systems in rural zones [9], and thus improving the business opportunities and prospects that can contribute to the development of the region. On the other hand, the principal disadvantage of the use of photovoltaic energies is the initial investment cost, which is, however, recoverable over time [10]. Moreover, the price of photovoltaic panels decreases continuously, making its use in different applications feasible. Today, monocrystalline silicon cell panels, for power generation and brushless motors, for water pumping, represent the most efficient and cost effective technology [11–17]. Some research projects have been undertaken specifically in isolated communities. In 2010, Gonzales conducted a project—*Photovoltaic, Pumping-System Prototype for Cooperation Projects towards Development with Appropriate Technologies* [18]—in which the author provided information regarding the installation of a particular water-pumping prototype whose energy is derived from photovoltaic panels, which feed the motor. He performed multiple simulation runs, changing parameters such as the need for maintenance of the system, so that its functioning could be optimized. The author concluded that the technology could be implemented in developing countries with a low quality of life, which was also affirmed by Sagahon [19]. In 2013, Perez presented a project—*Water-Pumping Systems Utilizing Photovoltaic, Solar Energy* [20]—for which the author performed an economic study regarding the utilization of photovoltaic energy for the pumping of water and addressing subjects as the necessary investment and the subsequent returns on investment of this kind of projects. The author proposed that legislation was updated so that private individuals could opt for this type of technology for the generation of electrical power. Cuadros et al. [21] presented a procedure for the simplified dimensioning and measurement of photovoltaic pumping systems, which he calls photo-irrigation.

The applications of photovoltaic energy are innumerable. Currently, the technology represents an alternative for the isolated communities, which lack energy resources. Nevertheless, in Latin America, the use of this technology has not been adequately promoted. The present project studies the performance of a photovoltaic pumping system in continuous current, evaluating its benefits and challenges.

3 Experimental Approach

3.1 Experimental Model. The present study aims to evaluate an experimental prototype consisting of a photovoltaic generation unit (*a* in Fig. 1), a pumping and storage unit (*b* in Fig. 1), and a data-acquisition unit (*c* in Fig. 1).

3.1.1 Photovoltaic Generation Unit. The photovoltaic generation unit is responsible for transforming solar energy into electrical power. It consists of a PV array and a controller. The characteristics of the PV array (Fig. 2) are described in Table 1.

The controller (Table 2) regulates the electrical power generated by the panels according to the requirements of the pump. The regulator is in charge of disconnecting the pump when there is not enough solar radiation to power the pumping system. The system
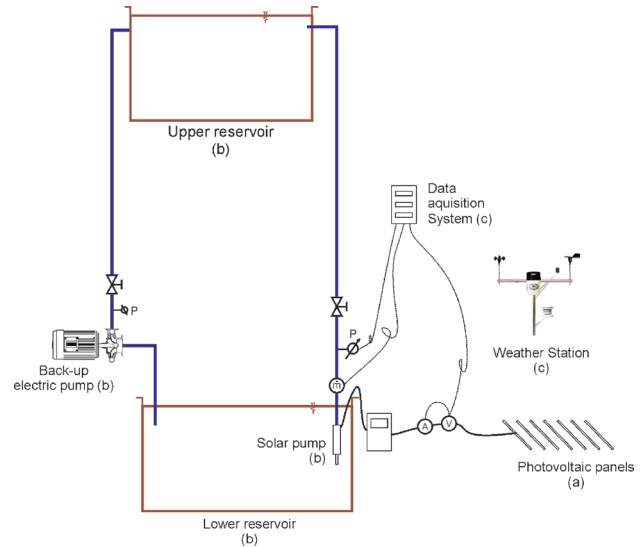

Fig. 1 Scheme of the experimental model

is automatically disconnected when available irradiance falls below 200 W/m^2. The power regulator controls and monitors the inputs in order to protect the system against dry running of the pump, reverse polarity, overload, and overheating. This is done using integrated maximum power point tracking (MPPT).

3.1.2 Pumping and Storage Unit. The hydraulic pump is responsible for the transformation of electrical power into mechanical power (electric motor) and then into hydraulic power (pump). It is an integrated, submergible motor (Table 3) coupled with a centrifugal pump (Table 4).

The pump is submerged in the lower reservoir (Fig. 1). It pumps the water to the upper reservoir (Fig. 1), from where it will be distributed to the agricultural plots through microdripping, due to the force of gravity.

3.1.3 Instrumentation and Data-Acquisition Unit. The meteorological station (VANTAGE PRO2 PLUS HOBO®) is made up of: (1) temperature and relative-humidity sensors, (2) a precipitation sensor, (3) a wind speed and direction sensor (0–50 m/s), and (4) a solar-radiation sensor, consisting of a cast acrylic diffuser, a photodiode, and signal-processing circuitry, housed in an anodized aluminum case (0–2000 W/m^2). All the received signals are sent to a data-acquisition system within the station itself, where they are stored every 10 min (Micro Station Data Logger—H21-002 HOBO). The station has been registering data since 2015.

For the energy assessment and the pumping system performance analysis, specialized sensors and a Data Logger Switch unit were used.

In order to measure the electrical current, an electrical shunt, which transforms the current in voltage into a relation of 1 A for 1 mV, was used. To measure the voltage (photovoltaic panels), a DC/DC transformer of 50 V to 1 V was used. The water flow mass measurement system was composed of a nozzle and a differential pressure transducer. The measuring principle is based on the concept stating that the pressure drop caused by the nozzle is proportional to the mass flow. The nozzle was manufactured in compliance with the ISO 5167-1 norm, with a beta (diameter relationship) of 0.5. The equipment responsible for measuring the pressure difference in the flow gauge was a differential-pressure traducer, which transforms the hydraulic pressure into a signal that varies from 4 mA to 20 mA. To measure absolute pressure in the exit of the pump, a traducer was used, with 0–100 m of water-column pressure corresponding to an output signal from 4 mA to 20 mA. The signals emitted by all the instruments were transferred to the data-acquisition system (34972 A LXI Data Acquisition Unit, Keysight Technologies). The data acquisition unit consisted

Fig. 2 Photovoltaic array

of a 60-channel, three-slot mainframe with a built-in 6 ½ digit multimeter. Each channel can be configured independently to measure one of 11 different parameters (i.e., DC voltage, alternating current (AC) voltage, resistance, frequency and period, DC current, true root-mean-square AC current, and temperature). The data-recording interval was 1 s.

The studied parameters were the following:

Solar irradiation

$$\dot{E} = \int I_s dt \tag{1}$$

$\dot{E}$ is the solar irradiation $\left(\text{W} \cdot \text{h/m}^2\right)$, I_s is the solar irradiance (W/m²), and t is the time.

Solar power

$$P_s = I_s \cdot A \tag{2}$$

Table 1   Characteristics of the PV array

Description	Value
Brand, model	INTIPOWER
PV module power	120 W (standard test conditions)
PV array area	52 m²
Cells type	Monocrystalline Si
PV array power	4 kW (standard test conditions)
Orientation and tilt angle of the PV array	N, 17 deg

Table 2   Characteristics of the controller

Description	Value
Brand, model	Lorentz, PS4000
Power	Maximum 4 kW
Input voltage	Maximum 375 V
Optimum voltage	> 238 V

Table 3   Characteristics of the motor

Description	Value
Brand, model	Lorentz, ECDRIVE 4000-C
Type	Brushless DC motor
Power	3.5 kW
Efficiency	Maximum 92%
Motor speed	900–3300 rpm
Submersion	Maximum 250 m

Table 4   Characteristics of the pump

Description	Value
Brand, model	Lorentz, PE C-SJ17-4
Power	3.5 kW
Type	Multistage
Stages	4
Submersion	Maximum 250 m

Table 5   Uncertainties

| Parameter	Uncertainty (%)	Reference
Solar irradiance	0.5	Instrument
Solar irradiation	0.5	$\left[\left(\dfrac{\delta t}{t}\right)^2 + \left(\dfrac{\delta I_s}{I_s}\right)^2\right]^{0.5}$
Electrical current	0.5	Instrument
Voltage	0.1	Instrument
Pressure	0.3	Instrument
Pressure difference	0.5	Instrument
Temperature	2.5	Instrument
Wind speed	4	Instrument
Relative humidity	5	Instrument
Solar power	0.6	$\left[\left(\dfrac{\delta A}{A}\right)^2 + \left(\dfrac{\delta I_s}{I_s}\right)^2\right]^{0.5}$
PV array power	0.5	$\left[\left(\dfrac{\delta A}{A}\right)^2 + \left(\dfrac{\delta I_s}{I_s}\right)^2\right]^{0.5}$
Mass flow	0.3	$\left[\dfrac{\delta \Delta P}{2 \cdot \Delta P}\right]$
Hydraulic power	0.4	$\left[\left(\dfrac{\delta \dot{m}}{\dot{m}}\right)^2 + \left(\dfrac{\delta \text{TDH}}{\text{TDH}}\right)^2\right]^{0.5}$
Efficiency of the PV array	0.8	$\left[\left(\dfrac{\delta P_{pv}}{P_{pv}}\right)^2 + \left(\dfrac{\delta P_s}{P_s}\right)^2\right]^{0.5}$
Hydraulic efficiency	0.6	$\left[\left(\dfrac{\delta P_h}{P_h}\right)^2 + \left(\dfrac{\delta P_{pv}}{P_{pv}}\right)^2\right]^{0.5}$
Global efficiency	0.7	$\left[\left(\dfrac{\delta P_h}{P_h}\right)^2 + \left(\dfrac{\delta P_s}{P_s}\right)^2\right]^{0.5}$
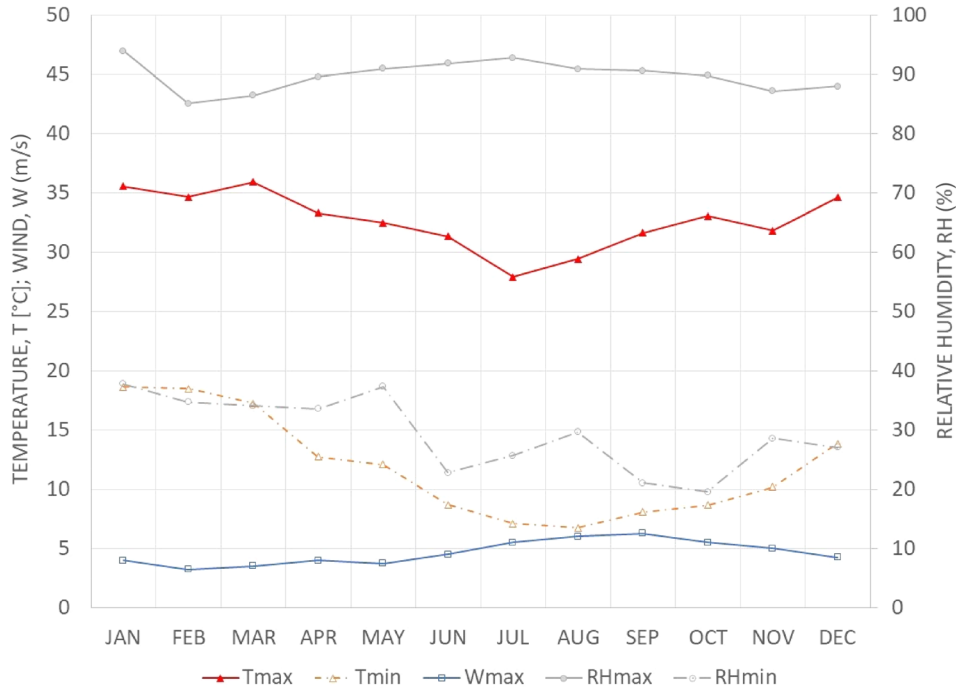
Fig. 3 Parameters monitored by the meteorological station

where P_s is the solar power (W), I_s is the solar irradiance (W/m^2), and A is the area of the PV array (m^2).

Electrical power of the PV array

$$P_{pv} = I_{pv} \cdot V_{pv} \qquad (3)$$

where P_{pv} is the PV array power (W), I_{pv} is the electrical current (A), and V_{pv} is the voltage (V).

Efficiency of the photovoltaic panels

$$\eta_{pv} = \frac{P_{pv}}{P_s} \qquad (4)$$

where η_{pv} is the efficiency of the PV array (W/W), P_{pv} is the PV array power (W), and P_s is the solar power (W).

Hydraulic power

$$P_h = g \cdot \dot{m} \cdot \text{TDH} \qquad (5)$$

where P_h is the hydraulic power (W), ρ is the fluid density (kg/m^3), g is the gravity (m/s^2), $\dot{m}$ is the mass flow (kg/s), and TDH is the total dynamic head (m).

Hydraulic efficiency

$$\eta_h = \frac{P_h}{P_{pv}} \qquad (6)$$

where η_h is the hydraulic efficiency (W/W), P_h is the hydraulic power (W), and P_{pv} is the PV array power (W).
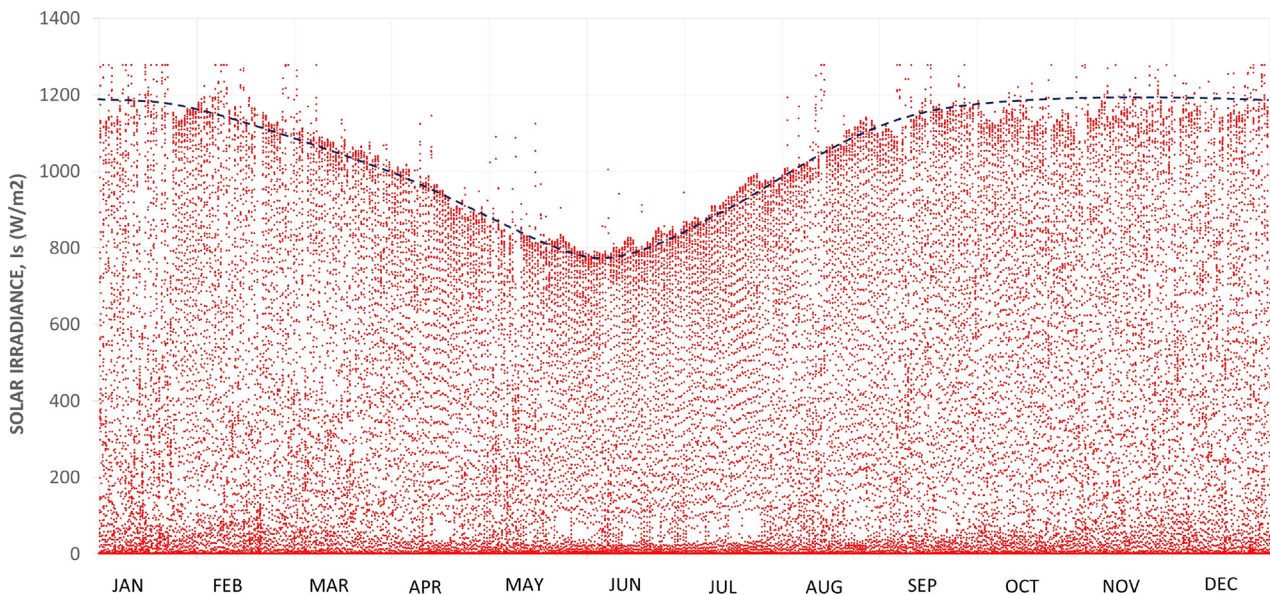
Global efficiency

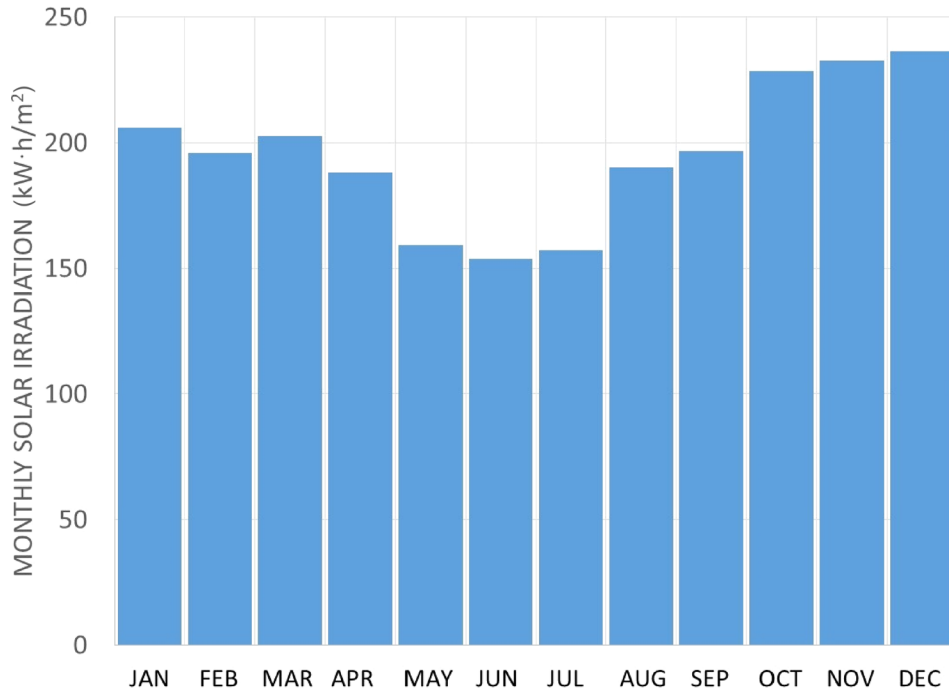**Fig. 4 Solar irradiancy for the year of 2017**

Fig. 5   Monthly solar irradiation

$$\eta_g = \frac{P_h}{P_S} \qquad (7)$$

where η_g is the global efficiency (W/W), P_h is the hydraulic power in (W), and P_s is the solar power (W).

3.2   Studied Uncertainties. The analysis of uncertainties was conducted under the criterion of "uncertainty propagation" [22]. The results are shown in Table 5.

4   Results

The results are divided into two parts: the energetic potential of the zone and the performance of the pumping system.

4.1   Meteorological Station. The maximum wind speed during the year 2017 was 6.3 m/s in the month of September (Fig. 3). The characteristics of the zone limit the energetic potential for wind-power generation. For this reason, any possibility regarding
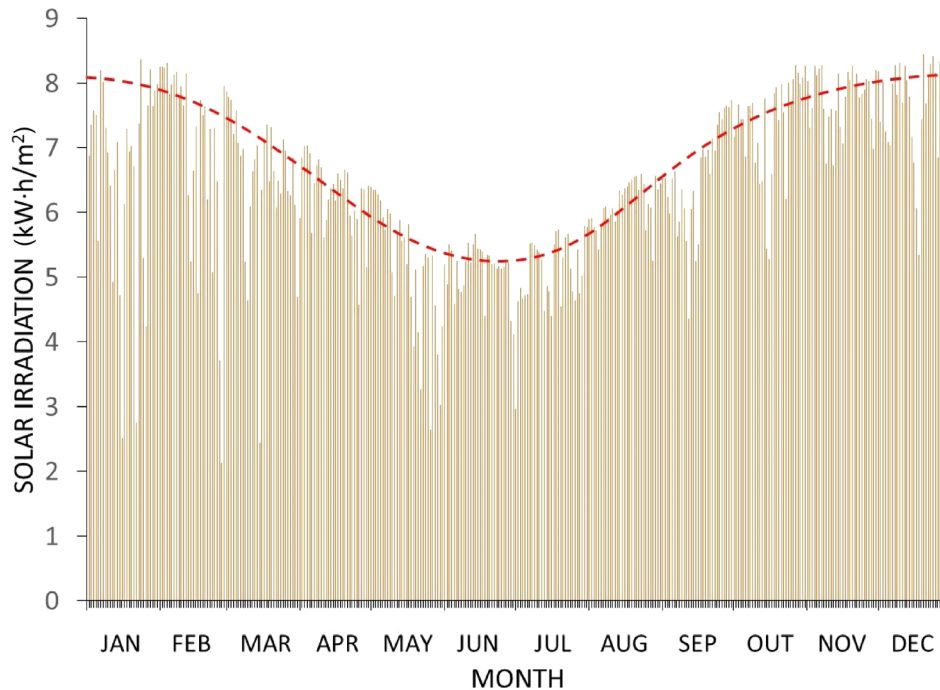

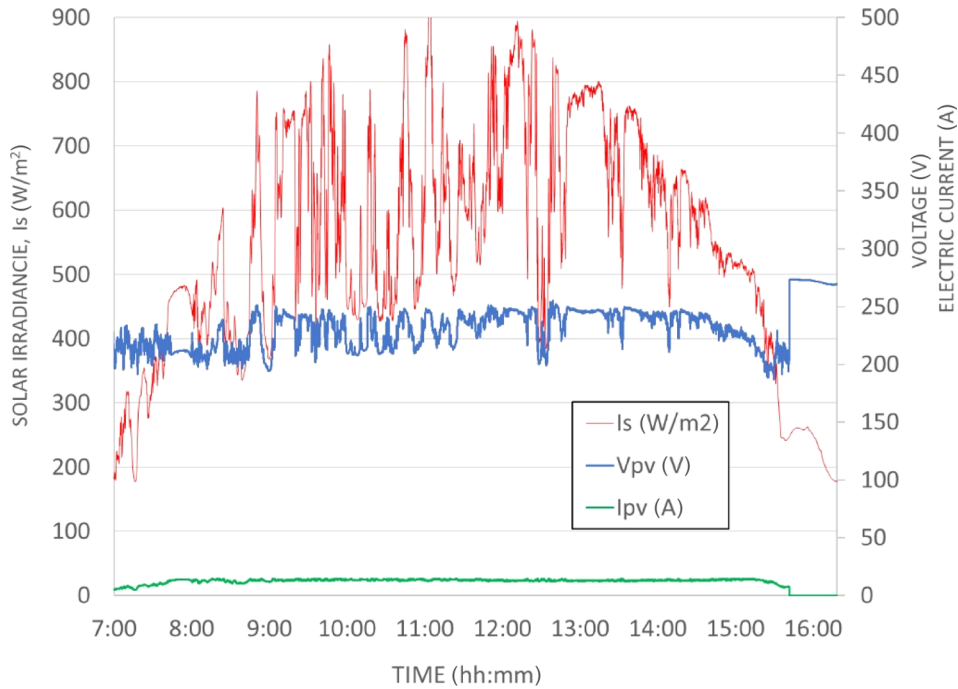**Fig. 6   Daily solar irradiation**

Fig. 7 Performance of the PV array

the exploitation of this particular method was not considered. The relative humidity according to the data obtained in the present research project throughout 2017 is identified in Fig. 3. It went from 94% in the month of January to 19.6% in October. In Fig. 3, temperature variation is indicated. It oscillates between 35.9 °C and 6.8 °C, the first being the highest temperature in January and the latest, the lowest in August. These temperature variations and relative humidity correspond to the typical climate of the southern valleys of Peru.

4.1.1 Solar Radiation. The solar radiation in the studied zone for the year of 2017 is presented in Fig. 4. Peak values between

$793.1 \, \text{W/m}^2$ and $1276.9 \, \text{W/m}^2$ were observed. The energetic potential of the zone is higher than the average of other locations in Latin America and the world.

The comparison of Figs. 3 and 4 shows that the highest solar irradiance values correspond to the highest ambient temperature values and that the lowest solar irradiance values correspond to the lowest ambient temperature values. These results confirm the seasonal climatic characteristics of southern Peru. This region benefits from an average of 300 sunny days per year and 8 sunlight hours per day, which are available for the harvesting of solar energy using different solar technologies, such as photovoltaic panels. The solar irradiation for the year of 2017 is shown in
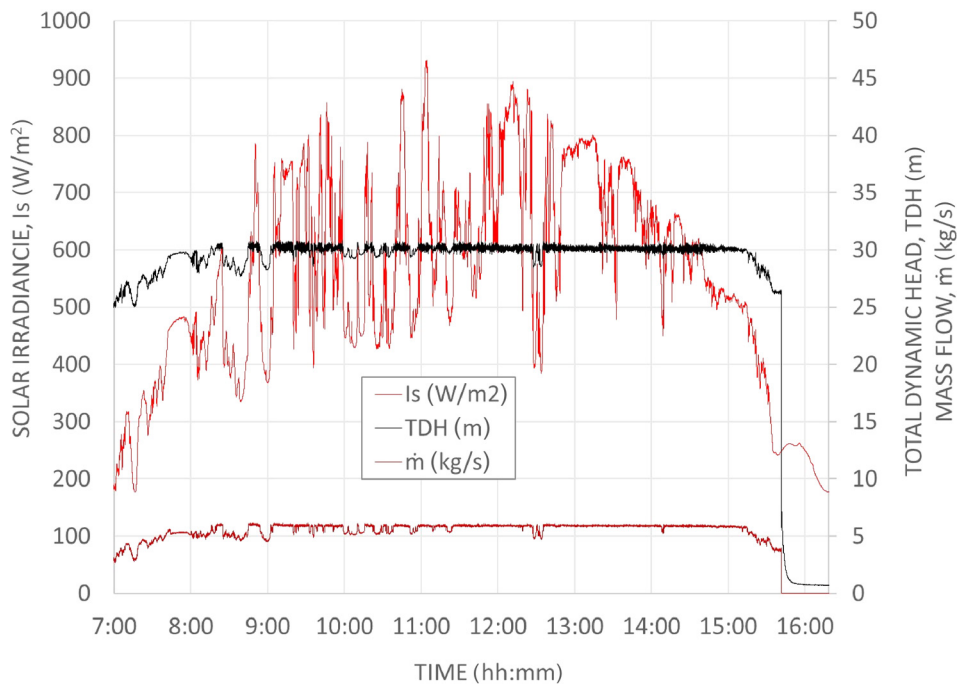

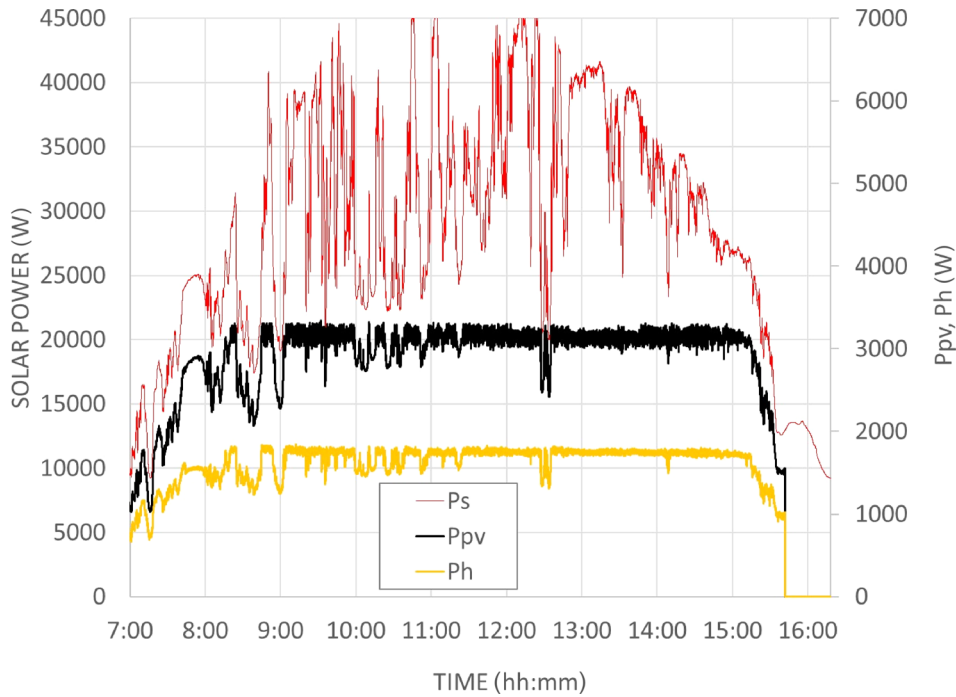**Fig. 8 Performance of the centrifugal pump**

Fig. 9   Solar power, electrical power of the PV array, and hydraulic power

Fig. 5. The maximum value of solar irradiation was $236 \, \text{kW·h/m}^2$ for the month of December and the minimum was $150 \, \text{kW·h/m}^2$ for June. These values were obtained through the integration of the data obtained from the pyranometer.

Figure 6 shows the daily solar irradiation for the year of 2017. The values vary from $5 \, \text{kW·h/m}^2$ to $8 \, \text{kW·h/m}^2$, which constitutes an important energy potential for the generation of power. These values are a proof of the influence of the Atacama Desert (northern Chile) in the southern Peru region, which has higher values than the rest of the Peruvian territory.

4.2   Performance of the Photovoltaic Solar Pumping System. Figure 7 shows the variation of solar irradiance and the corresponding PV array voltage and electric current for *a typical winter day* (June–July), for which peak solar irradiance (between 11 h and 12 h) reaches low values ($820 \, \text{W/m}^2$ approximately) compared to the rest of the year. The stability of both current and voltage can be appreciated, despite variations in solar irradiance. Figure 7 also shows that although solar radiation is low in the early hours of the morning and in the late afternoon, the electrical parameters (electric current and voltage) are constant and allow the system to pump water.
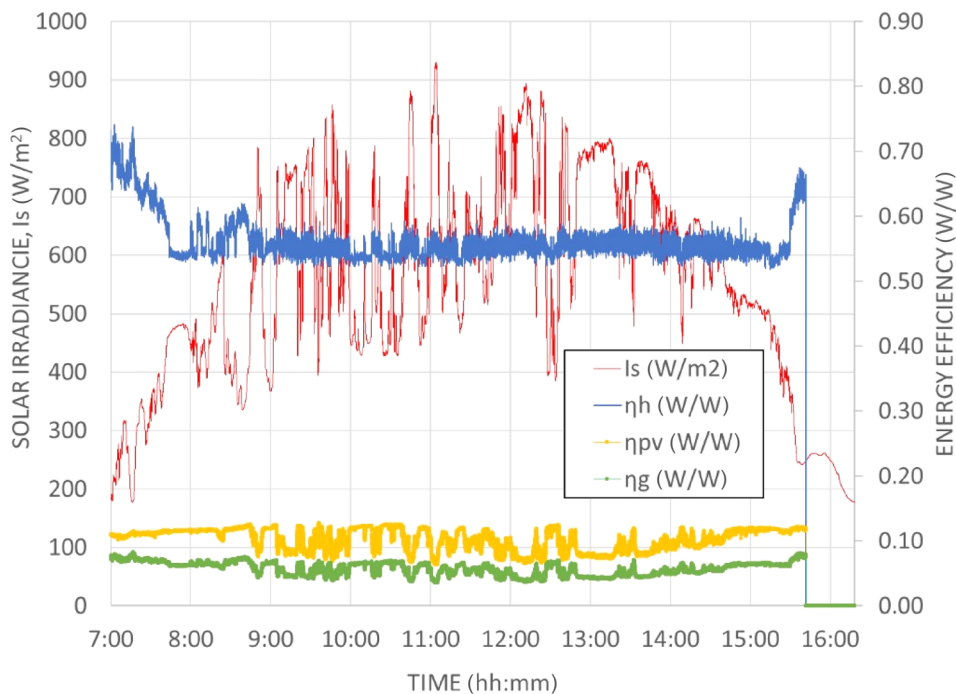

Fig. 10   Photovoltaic array Efficiency, hydraulic efficiency, and global efficiency
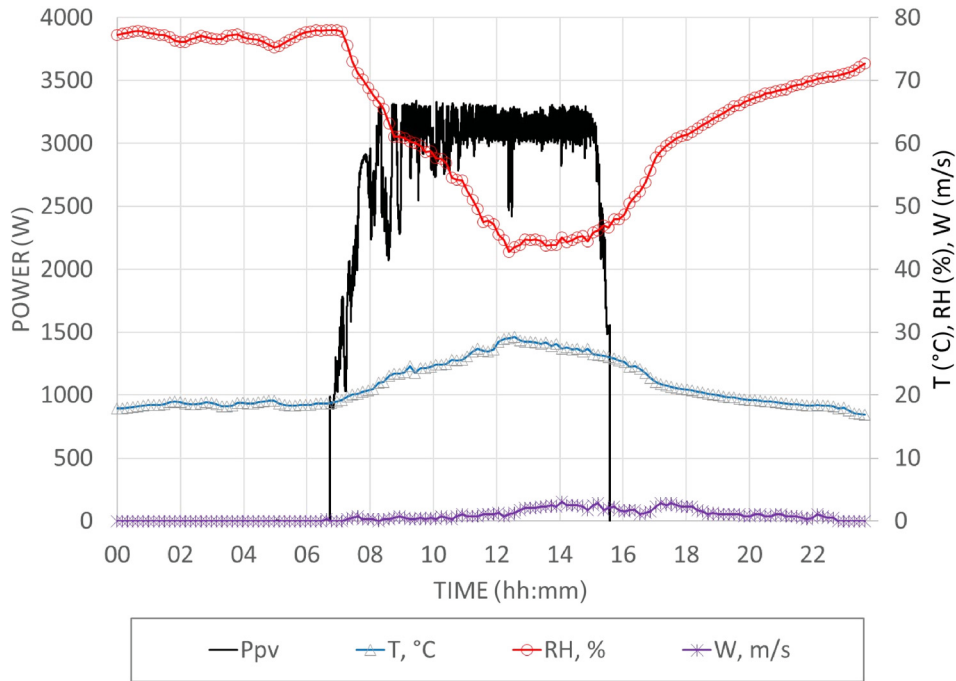
Fig. 11 Photovoltaic array power versus temperature, relative humidity, and wind speed

Figure 8 shows that the hydraulic parameters of the solar pump, i.e., total dynamic heat and mass flow, remain constant despite oscillations in solar radiation. Moreover, the pump possesses progressive starting and shutoff mechanisms, which increase its durability and reduce the necessity of maintenance of its components. The system works with a solar irradiance equal or superior to 200 W/m². When solar irradiance falls below these values, the system shuts down in order to avoid wearing of the components with a significantly reduced water flow.

The parameters shown in Fig. 8 demonstrate that the MPPT system allows for the exploitation of solar energy from the early hours of the morning until late afternoon (from 7 h 30 to 15 h 30), despite working with a minimum peak solar irradiance (820 W/m² approximately). Average values of 30 m (THD) and 5 kg/s (mass flow) were observed for this typical winter day.

Figure 9 shows the power provided by the sun (P_s), the photovoltaic array power (P_{pv}), and the hydraulic power produced by the electro-pump (P_h). The power of the panels and hydraulic power remained constant in the test that was conducted. Figure 9 shows also that the solar power is vastly superior to the power generated by the panels: only 12% of the solar power is transformed into electrical power. This yield corresponds to the
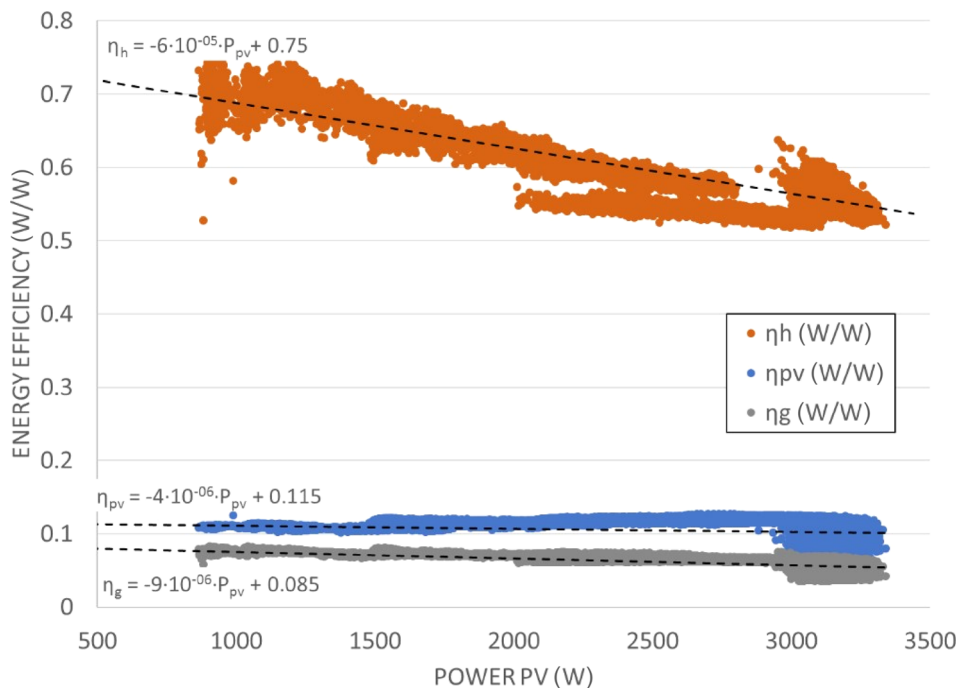

Fig. 12 Efficiencies of the photovoltaic system during the year of 2017
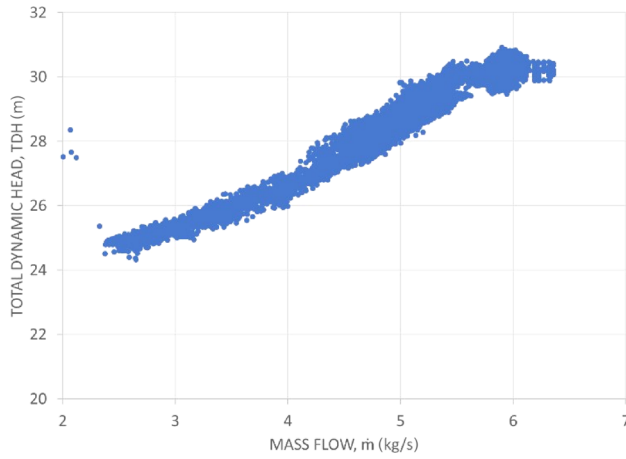
Fig. 13   Total dynamic head versus mass flow

monocrystalline PV panel technology. Higher performances can be attained with other PV technologies, but these alternatives would not be economically viable. Monocrystalline technology becomes everyday more accessible, which increases the feasibility of these kinds of projects.

Figure 10 shows the efficiency of the PV array. For the conducted test, the efficiency of the PV array reached 12%. However, this value is lower than the efficiency attained in laboratory functioning in the same conditions (17%). It is thought that the losses caused by conductors and the parallel-series configuration reduce the overall performance of the photovoltaic array.

The hydraulic efficiency was 55% approximately. For multistage, centrifugal electro-pumps, this is an adequate functioning value, which can be attained due to the "brushless" technology and the cooling system, i.e., the unit's immersion in water. The global efficiency of the system is around 6.5%; this value is mainly affected by the efficiency of the photovoltaic panels.

Due to the fact that the system functions only in DC, the efficiency results are superior to those observed in systems with DC/AC inversion [1,7,8,10,11,23]. However, the main advantage of these systems is the enhanced exploitation of solar energy. Systems with DC/AC current inverters function optimally in periods of high solar irradiance, generally up to 5 h per day. On the other hand, DC/DC systems can optimally harvest solar energy up to 8 h per day. The harnessing of solar energy at the beginning of the day and at the end of the afternoon allows for the pumping of water in smaller quantities, which is highly practical for irrigation in zones where there is a shortage of water.

Figure 11 shows the variation of the electrical power generated by the PV array with relation to the climate characteristics, i.e., relative humidity, dry-bulb temperature, and wind speed. The results show the strong influence of the MPPT system, which allows for the generation of continuous power despite solar irradiance oscillations. The performance of the PV system does not seem to be affected by temperature variations (from 19 °C to 30 °C), wind speed in the zone (from 0 m/s to 5 m/s), or relative humidity (from 43% to 88%). The MPPT system control electronics probably absorb the temperature effects, mainly in the PV system, not allowing the effects to impact the system's efficiency. Determining the influence of temperature in the performance of the PV system was not considered an objective of the current study; hence, specific tests were not conducted. However, the literature shows that PV power generation efficiency improves when PV systems are cooled.

Figure 12 shows the *performance of the PV array during the year of 2017*. The efficiency of the PV array, hydraulic, and global was evaluated with respect to the PV power generated. This allows for the interpretation of efficiency independent of solar irradiance. The efficiency of the PV array and global efficiency remained constant (11.5% and 8.5%, respectively). The functioning interval of the PV array ranges from 880 W up to 3400 W, making evident the versatility of the system of generation and consumption in DC, which is able to function since solar irradiance is at least 200 W/m^2, which corresponds to 880 W of PV array power, 27 m of TDH and 2 kg/s of mass flow, and 70% hydraulic efficiency. With greater mass flows (6.3 kg/s), the PV
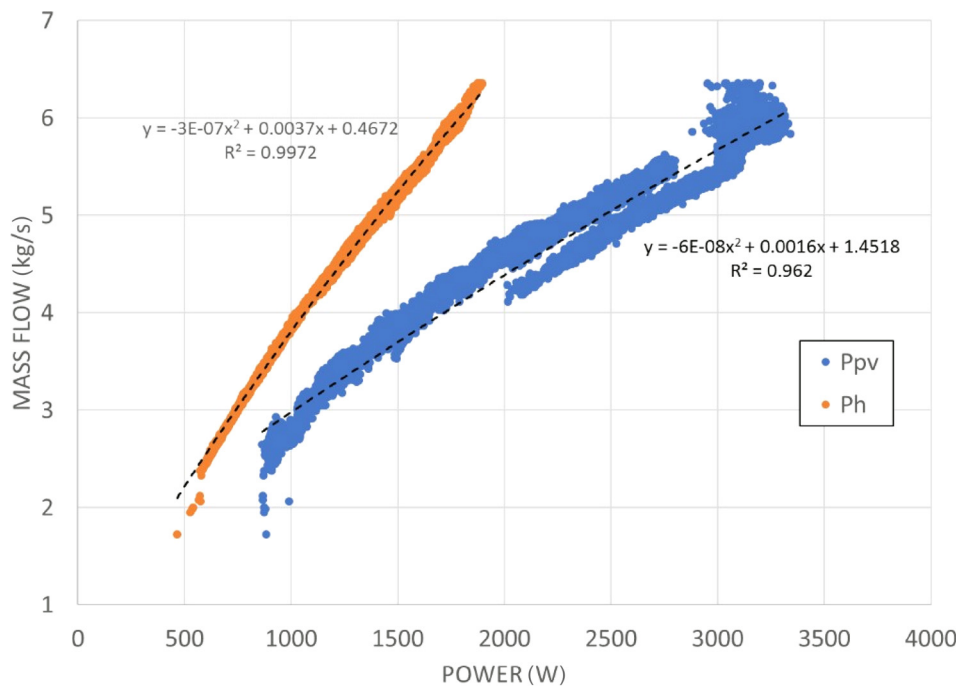

$$y = -3E\text{-}07x^2 + 0.0037x + 0.4672$$
$$R^2 = 0.9972$$

$$y = -6E\text{-}08x^2 + 0.0016x + 1.4518$$
$$R^2 = 0.962$$

Fig. 14   Flow mass versus power

array power was 3256 W with a hydraulic efficiency of 55%, a TDH of 30 m, and a peak solar irradiance of 1190 W/m^2; these are the conditions of the system during a month of maximum solar potential (from October to December), which would almost correspond to standard test conditions.

4.3 Performance of the Submergible Motor and Centrifugal Pump System. The results obtained from tests conducted on the hydraulic, electric motor–pump system during 2017 are shown in Fig. 13. The variation of TDH and mass flow can be observed. This graphic determines the working conditions of the pump in different solar irradiance conditions. For different TDH, the control system seeks to optimize energy management in such a way that it does not provide maximum mass flow but rather a percentage of it. Thereby, the system pumps from 2.4 kg/s (25 m of TDH) to 7.7 kg/s (30 m of TDH).

Figure 14 shows the variation of hydraulic power and mass flow, which is almost linear and proportional. According to the extrapolations in the same graphic, for maximum PV power (in conditions of maximum solar radiation), the maximum flow is 6.3 kg/s and the estimated hydraulic power is 1880 W (within the performance of the pump). These results agree with those of Tiwari and Kalamkar [23]. Figure 14 also shows that the pump can start functioning with a mass flow of 2 kg/s, which corresponds to a hydraulic power of 505 W.

The variation of mass flow and PV array power is also presented. The PV system functions from 880 W to 3310 W of PV power, which correspond to a mass flow of 2 kg/s and 6.3 kg/s, respectively: These results are in accordance with those of Tiwari and Kalamkar [23].

5 Conclusions

An experimental study was performed to analyze the generation of electrical power, using a photovoltaic system in continuous current to power a centrifugal water pump. The present research project reached the following conclusions:

- The energetic potential of the location of Uraca—Castilla, Arequipa, Peru, was determined. The specific zone where the project was undertaken is apt for the installation of photovoltaic systems, allowing for the harnessing of renewable resources, as well as the reduction of pollutant gas emissions.
- For the current for a typical winter day (June–July), the efficiency of the PV array reached 12%, the hydraulic efficiency was 55% approximately, the global efficiency of the system is around 6.5%.
- During the year of 2017, the system operated from 07 h 30 min to 15 h 30 min, with an average of 8 h a day during 300 days per year. The efficiency of the PV array and global efficiency remained constant (11.5% f and 8.5%, respectively). The functioning interval of the PV array ranges from 880 W up to 3400 W, which is able to function since solar irradiance is at least 200 W/m^2, corresponding to 880 W of PV array power, 27 m of TDH and 2 kg/s of mass flow, and 70% hydraulic efficiency. With greater mass flows (6.3 kg/s), the PV array power was 3256 W with a hydraulic efficiency of 55%, a TDH of 30 m, and a peak solar irradiance of 1190 W/m^2.
- This study shows the feasibility of implementing solar pumping systems to extend agricultural zones to isolated rural areas that lack resources. Projects of this kind can be replicated in similar environmental conditions.

Nomenclature

A = area (m^2)
$\dot{E}$ = solar irradiation (W · h/m^2)
g = gravity (m/s^2)
I_s = solar irradiance (W/m^2)
I_{pv} = electrical current (A)
$\dot{m}$ = mass flow (kg/s)
P_h = hydraulic power (W)
P_s = solar power (W)
P_{pv} = PV array power (W)
t = time
T = temperature (°C)
TDH = total dynamic head (m)
V_{pv} = voltage (V)
W = wind speed (m/s)
δ = uncertainty (prefix)
ΔP = differential pressure (Pa)
η_g = global efficiency (W/W)
η_h = hydraulic efficiency (W/W)
η_{pv} = efficiency of the PV array (W/W)
ρ = fluid density (kg/m^3)

Acronyms

AC = alternating current
DC = direct current
MPPT = maximum power point tracking
PV = photovoltaic
TDH = total dynamic head

References

[1] Azzedine, B., Hanini, S., and Arab, A. H., 2017, "Performances' Investigation of Different Photovoltaic Water Pumping System Configurations for Proper Matching the Optimal Location, in Desert Area," Energy Convers. Manage., **151**, pp. 439–456.
[2] Tiwari, A. K., and Kalamkar, V. R., 2017, "Effects of Total Head and Solar Radiation on the Performance of Solar Water Pumping System," Renewable Energy, **118**, pp. 919–927.
[3] Patil, V. R., Biradar, V. I., Shreyas, R., Garg, P., Orosz, M. S., and Thirumalai, N. C., 2017, "Techno-Economic Comparison of Solar Organic Rankine Cycle (ORC) and Photovoltaic (PV) Systems With Energy Storage," Renewable Energy, **113**, pp. 1250–1260.
[4] SENAMHI, DEP-MEM, 2013, "Atlas de Energía Solar del Perú, Proyecto PER/98/G31 Electrificación Rural a Base de Energía Fotovoltaica en el Perú," Ministerio de Energía y Minas, Lima, PE.
[5] Raman, P., Murali, J., Sakthivadivel, D., and Vigneswaran, V., 2012, "Opportunities and Challenges in Setting Up Solar Photovoltaic Based Micro Grids for Electrification in Rural Areas of India," Renewable Sustainable Energy Rev., **16**(5), pp. 3320–3325.
[6] Ghoneim, A., 2006, "Design Optimization of Photovoltaic Powered Water Pumping Systems," Energy Convers. Manage., **47**(11–12), pp. 1449–1463.
[7] Babkir, A., 2017, "Comparative Assessment of the Feasibility for Solar Irrigation Pumps in Sudan," Renewable Sustainable Energy Rev., **81**(1), pp. 413–420.
[8] Mohammad, A.-S., 2012, "Application of Photovoltaic Array for Pumping Water as an Alternative to Diesel Engines in Jordan Badia, Tall Hassan Station: Case Study," Renewable Sustainable Energy Rev., **16**(7), pp. 4500–4507.
[9] Hamidat, A., and Benyoucef, B., 2009, "Systematic Procedures for Sizing Photovoltaic Pumping System, Using Water Tank Storage," Energy Policy, **37**(4), pp. 1489–1501.
[10] Chueco-Fernández, F., and Bayod-Rújula, Á., 2010, "Power Supply for Pumping Systems in Northern Chile: Photovoltaics as Alternative to Grid Extension and Diesel Engines," Energy, **35**(7), pp. 2909–2921.
[11] Chandel, S., Nagaraju, M., and Chandel, R., 2015, "Review of Solar Photovoltaic Water Pumping System Technology for Irrigation and Community Drinking Water Supplies," Renewable Sustainable Energy Rev., **49**, pp. 1084–1099.

[12] Fernández, E. C., 2009, "Energía Solar Fotovoltaica, Competitividad y Evaluación Económica, Comparativa y Modelos," Ph. D. thesis, Madrid, Spain.

[13] García, J. M., 2011, "Desarrollo de un Controlador para Motores DC brushless Basado en CompactRIO y LabVIEW de National Instruments para el Estudio de Nuevos Algoritmos de Control," Universidad Carlos III de Madrid, Madrid, Spain.

[14] Escobar, F., Martinez, A., and Tèllez, A., 2005, "Control de un Motor Brushless DC con Frenado Regenerativo," Pontificia Universidad Javeriana, Bogota, Colombia.

[15] Gouws, R., and Lukhwareni, T., 2012, "Factors Influencing the Performance and Efficiency of Solar Water Pumping System: A Review," Int. J. Phys. Sci., **7**(48), pp. 6169–6180.

[16] Li, G., Jin, Y., and Chen, X., 2017, "Research and Current Status of the Solar Photovoltaic Water Pumping System—A Review," Renewable Sustainable Energy Rev., **79**, pp. 440–458.

[17] Swan, L. G., and Allen, P. L., 2010, "Integrated Solar Pump Design Incorporating a Brushless DC Motor for Use in a Solar Heating System," Renewable Energy, **35**(9), pp. 2015–2026.

[18] Arija, D., 2010, "Prototipo de Sistema de Bombeo Fotovoltaico para Proyectos de Cooperación al Desarrollo de Tecnologías Apropiadas," Universidad Carlos III de Madrid, Madrid, Spain.

[19] Sagahon, P., and Atahualpa, I., 2013, "Energía Solar Térmica y Fotovoltaica Aislada para Pequeñas Comunidades en Perú," Universidad Politecnica de Catalunya, Catalonia, Spain.

[20] Correia, M. C., 2015, *Tesis de Sistemas de Bombagem de Água Utilizando Energia Solar Fotovoltaica*, Instituto Superior de Enghenaria de Lisboa, Lisboa, Portugal.

[21] Cuadros, F., Lopez-Rodriguez, F., and Marcos, A., 2004, "A Procedure to Size Solar-Powered Irrigation (Photoirrigation) Schemes," Sol. Energy, **76**(4), pp. 465–473.

[22] Moffat, R. J., 1988, *Describing the Uncertainties in Experimental Results*, Stanford University, Stanford, CA.

[23] Tiwari, A. K., and Kalamkar, V. R., 2016, "Performance Investigations of Solar Water Pumping System Using Helical Pump Under the Outdoor Condition of Nagpur, India," Renewable Energy, **97**, pp. 737–745.